Preparation and electrical conductivity of $(Cu_{0.5}Ag_{0.5})_7SiS_5I$-based superionic ceramics

I.P. Studenyak [a, *], A.I. Pogodin [a], I.A. Shender [a], S.M. Bereznyuk [a], M.J. Filep [a], O.P. Kokhan [a], P. Kúš [b]

[a] *Uzhhorod National University, Pidgirna St. 46, Uzhhorod, 88000, Ukraine*
[b] *Comenius University, Mlynska Dolina, Bratislava, 84248, Slovakia*

ARTICLE INFO

ABSTRACT

The ceramics based on $(Cu_{0.5}Ag_{0.5})_7SiS_5I$ solid solution of superionic conductor with argyrodite structure were prepared by using the powders with different particles size. The structural studies of powders were performed by XRD technique, while the ceramic samples with different average size of the crystallites were investigated by microstructural analysis. The total electrical conductivity of ceramic samples was measured by impedance spectroscopy in the frequency range from 10 Hz to 2×10^6 Hz and temperature interval from 292 K to 383 K. The contributions of ionic and electronic components into the total electrical conductivity were separated as well as their temperature behavior was studied. The dependences of ionic and electronic conductivity and their activation energies on average size of the crystallites in $(Cu_{0.5}Ag_{0.5})_7SiS_5I$-based ceramic samples were investigated.

© 2020 Elsevier B.V. All rights reserved.

1. Introduction

Among ceramic materials, electrochemical ceramics have recently been widely studied in order to develop the latest technologies of electrochemical energy storage, which is caused by the rapid development of alternative energy sources, electric vehicles and portable electronic devices [1–5]. Electrochemical capacitors (supercapacitors), batteries and fuel cells are usually used as electrochemical energy storage devices [2]. The most promising materials in this regard are solid electrolytes used in all-solid-state batteries. It should be noted that the use of solid electrolyte instead of liquid one not only increases the safety of batteries, but also simplifies the design of the battery itself [5–8].

Since the efficiency of batteries directly depends on the properties of the working material, so the search for and improvement of new materials is relevant. Sulfur-containing solid electrolytes attract considerable attention due to the high ionic conductivity, which is provided by the peculiarities of their crystal structure [5,6,9–12], among which it is worth noting complex phosphorus sulfides with Li^+ and Na^+. Usually sulfur-containing superionic

compounds with ionic conductivity of Li^+ and Na^+ are difficult to obtain in the crystalline state [11], so they are obtained in glass-ceramic form [10,11,13,14].

It should be noted that promising superionic materials in this regard are presented by compounds with the structure of argyrodite [15–18], which have high values of ionic conductivity. They are characterized by a similar crystalline structure (tetrahedral dense packaging) and high variability of compositions [19,20], which favors the formation of solid solutions. The compounds with argyrodite structure are characterized by the presence of a rigid anionic framework, the basis of which is a tetrahedron $[SiS_4]$ and polyhedra $[S_3I]$ and $[SI_4]$ [20]. From the above-mentioned tetrahedra, icosahedra are formed, which are coordinated around a sulfur or selenium atom, which is the top of both $[SiS_4]$ tetrahedra and also the top of the next icosahedron $[SS_9I_3]$, due to the interpenetration of icosahedra. In addition, double tetrahedra $[Cu(Ag)S_3I_2]$ formed by sulfur atoms S1, S2 and atom I1 can be distinguished in the elementary cell. It is these double polyhedra that are coordinated around the moving positions of Cu (Ag), from which the moving cationic sublattice is formed. As the most mobile Cu (Ag) positions are considered that have a triangular coordination or are located on the edges of the polyhedra of the anionic framework [20].

In addition, in recent years the argyrodites have been obtained

in the forms of composites, ceramics and thin films [21−24]. Copper-containing argyrodites in ceramic form were studied in Ref. [23]. In this paper, we will focus on investigating new ceramic material $(Cu_{0.5}Ag_{0.5})_7SiS_5I$ based on argyrodites, in which half of the copper atoms are replaced by silver atoms. As far as we know nowadays, such studies have not been performed. The electrical properties of $(Cu_{0.5}Ag_{0.5})_7SiS_5I$, obtained in the form of a single crystal by the method of directional crystallization from the melt, were studied by impedance spectroscopy in Ref. [25]. In present paper, the electrical properties of ceramic samples based on $(Cu_{0.5}Ag_{0.5})_7SiS_5I$ compound are investigated. The production of solid electrolytic batteries in the form of ceramic samples is caused by significant advantages (compared to the cultivation of single crystals) in terms of practical application due to ease of production (lower annealing temperatures and annealing times, the ability to manufacture material of precisely defined geometric size and shape, etc.), manufacturability and economy. The presented paper shows the results of research on ceramic samples (after annealing) obtained from micro- and nanocrystalline powders. The choice of the chemical composition of ceramics based on $(Cu_{0.5}Ag_{0.5})_7SiS_5I$ is justified by the fact that it most clearly characterizes a solid solutions, it has half the copper atoms substituted by silver atoms and is characterized by the highest degree of compositional disorder.

Thus, this paper focuses on recrystallization of micro- and nanocrystalline powders in the annealing process, measurement of total electrical conductivity (with further separation into ionic and electronic components), study of dimensional effect in the obtained ceramic samples, which allows to predict their operational characteristics. This determines the scientific novelty and relevance of the study of the electrical properties of superionic ceramics based on $(Cu_{0.5}Ag_{0.5})_7SiS_5I$. Besides, the aim of this paper is to compare the electrical parameters of the obtained ceramic samples with the parameters of crystals.

2. Methods

$(Cu_{0.5}Ag_{0.5})_7SiS_5I$ solid solution was synthesized from pre-synthesized Cu_7SiS_5I and Ag_7SiS_5I compounds in vacuumized quartz ampoules. The process of $(Cu_{0.5}Ag_{0.5})_7SiS_5I$ synthesis included step heating up to 1023 K at a rate of 100 K/h and ageing during 48 hours, further increase of temperature to 1470 K at a rate of 50 K/h and ageing at this temperature for 72 hours. The annealing temperature was 873 K, ageing at this temperature for 120 hours. Cooling to room temperature was performed in the oven off mode.

The ceramic samples were prepared from powders of different dispersion: 1) powders obtained by grinding in an agate mortar with an average particle size of ~10−50 μm; 2) powders obtained by grinding in a planetary ball mill PQ-N04 for 30 min and 60 min with a speed of 200 rpm. Then the powders were pressed at ~400 MPa and were annealed at 973 K during 36 hours. In such a way the polycrystalline ceramic samples were fabricated in the form of disks with a diameter of 8 mm and a thickness of 3−4 mm.

The structural properties of $(Cu_{0.5}Ag_{0.5})_7SiS_5I$ powders and ceramic samples were studied by XRD technique and microstructural analysis. The XRD measurements were performed be the diffractometer DRON 4−07 with CuKα radiation, angle scanning speed 2θ was 0.02°, exposure was 1 s. The ceramic samples were investigated by microstructural analysis using metallographic microscope METAM - R1.

Electrical conductivity measurements were carried out by impedance spectroscopy [26] in frequency range from 10 Hz to 2×10^6 Hz and temperature interval from 292 to 383 K ranges with combination of high-precision LCR meters: Keysight E4980A and

AT-2818. The amplitude of the alternating current constituted 10 mV. Measurement was carried out by a two-electrode method, on blocking (electronic) gold contacts. Gold contacts for measurements were applied by chemical precipitation from solutions [25].

3. Results and discussion

Fig. 1 shows the XRD patterns for $(Cu_{0.5}Ag_{0.5})_7SiS_5I$ powders with different average particle size. It is shown that XRD patterns for $(Cu_{0.5}Ag_{0.5})_7SiS_5I$ powders are similar to diffractogram for $(Cu_{0.5}Ag_{0.5})_7SiS_5I$ solid solution crystal [25]. Comparison of diffractograms indicates that the lines broadening occurs with particle size decrease (Fig. 1). The results of microstructural analysis for prepared $(Cu_{0.5}Ag_{0.5})_7SiS_5I$-based ceramics are presented in Fig. 2. From histograms of crystallites size distribution for different ceramic samples, obtained from powders which grinding in agate mortar and planetary ball mill for 30 min and 60 min, the size of crystallites after annealing was determined (Fig. 2).

It is shown that the ceramic samples prepared by sintering powders obtained by grinding in a planetary ball mill are characterized by a more homogeneous microstructure, characterized by the distribution of particles in a narrower range, in contrast to the samples obtained by sintering a microcrystalline powder with a particle size of 10−50 μm (Fig. 2). As a result of recrystallization process, the average size of crystallites for samples obtained from powders grinding in an agate mortar is ~12 μm, while for samples obtained from powders grinding in a planetary ball mill for 30 min and 60 min is ~5 μm and ~3 μm, respectively.

Fig. 3 presents the frequency dependences of total electrical conductivity for $(Cu_{0.5}Ag_{0.5})_7SiS_5I$-based ceramics. With frequency increase the electrical conductivity grows which is typical for materials with ionic conductivity in solid state [27]. The insert to Fig. 3 shows the dependence of the total electrical conductivity on the size of crystallites. It is revealed that at decrease of size of crystallites from 12 μm to 3 μm the decrease of total electrical conductivity for $(Cu_{0.5}Ag_{0.5})_7SiS_5I$-based ceramic samples is observed.

For separation of the total electrical conductivity into ionic and electronic components, a standard approach using electrode equivalent circuits (EEC) [27,28] and their analysis on Nyquist plots was used. The parasitic inductance of the cell (~2×10^{-8} H) is taken into account during the analysis of all ceramic samples. It is shown that ceramic samples prepared on the basis of $(Cu_{0.5}Ag_{0.5})_7SiS_5I$, are characterized by equal values of electronic and ionic components of electrical conductivity ($\sigma_{ion}\sigma_{el}$). At Z′-Z″ dependences for $(Cu_{0.5}Ag_{0.5})_7SiS_5I$-based ceramics with average crystallites size of 12 μm, 5 μm, and 3 μm two semicircles are observed.

The EEC, which described the Nyquist plots, can be divided in two parts: one of them relates to ionic processes, another one to electronic processes. Low-frequency semicircles on the Nyquist plots correspond to the diffusion relaxation processes at the electrode/crystal boundary which is described by the capacity of the double diffusion layer C_{dl} and Warburg element of W_d, responsible for diffusion within the latter (Fig. 4). Serial to them were included the elements with R_{gb}/C_{gb} parameters which related to resistance and capacity of the grain boundaries of ceramic samples (the end of low-frequency semicircles) (Fig. 4). High-frequency semicircles correspond to the conductivity processes determined by the resistance of intra-grain boundaries, which is marked by R_{db} on the EEC (Fig. 4). Thus, the ionic conductivity of $(Cu_{0.5}Ag_{0.5})_7SiS_5I$-based ceramic samples is determined by the sum of the resistance of grain boundaries R_{gb} and the resistance limiting the ion diffusion W_R. It should be noted that on EEC parallelly to the elements responsible for ion processes the electronic resistance R_e is included and determined electronic conductivity of the samples (Fig. 4). With crystallites size decrease (12 μm →5 μm→ 3 μm) the low-
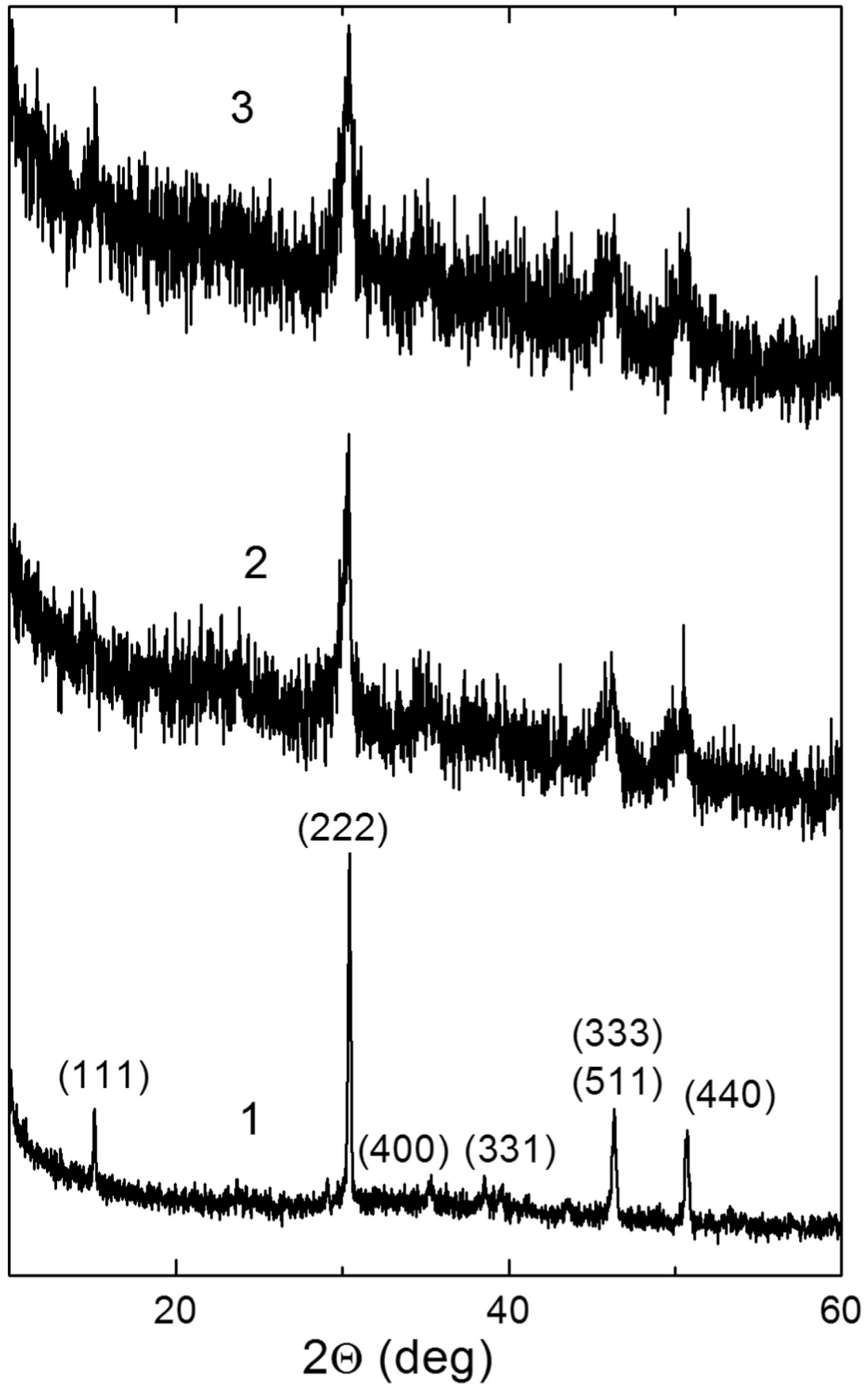
Fig. 1. Diffractograms of $(Cu_{0.5}Ag_{0.5})_7SiS_5I$ powders obtained by grinding in agate mortar (1) and planetary ball mill for 30 min (2) and 60 min (3).
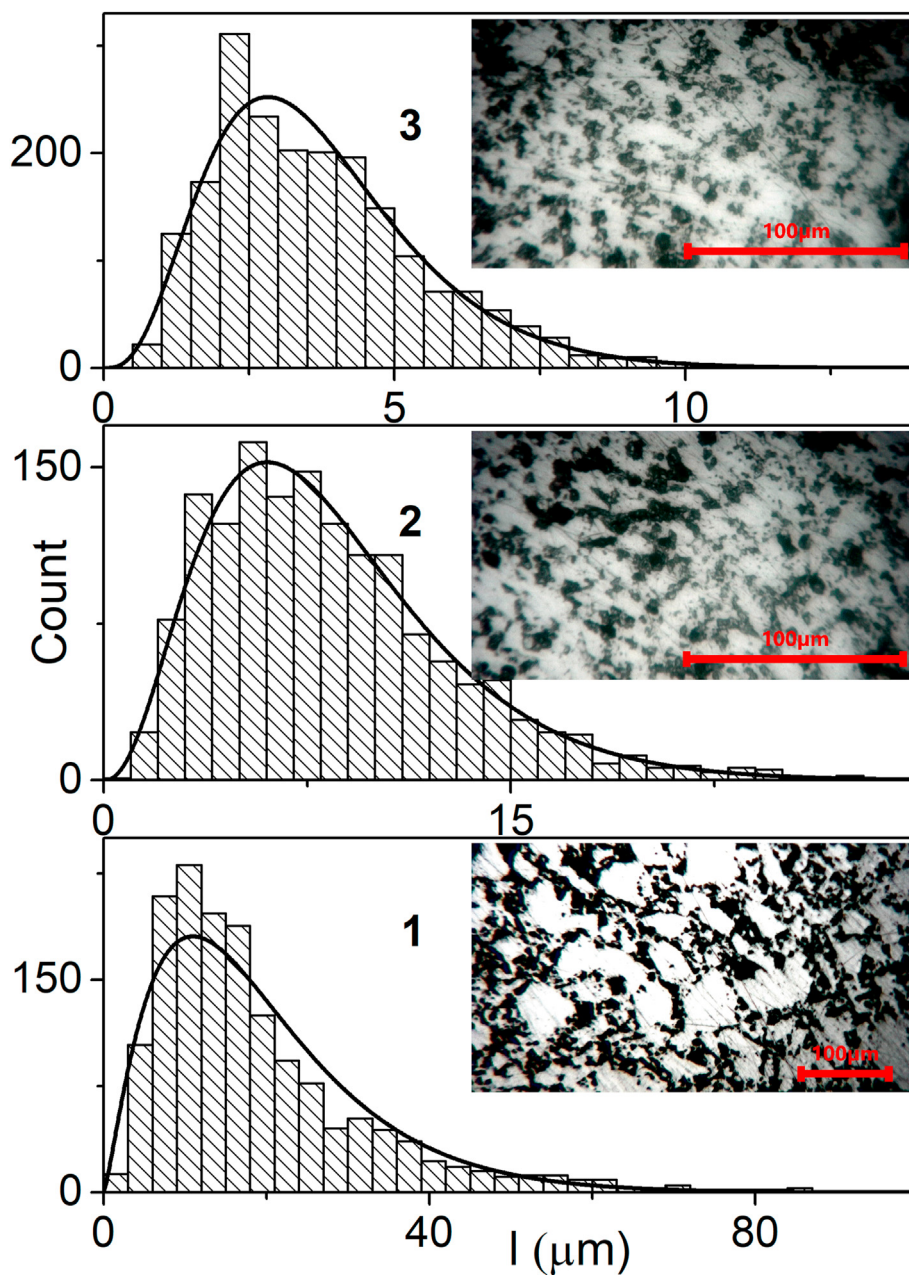
Fig. 2. Dependences of size distribution for crystallites of $(Cu_{0.5}Ag_{0.5})_7SiS_5I$ ceramic samples, obtained from powders which were milled in agate mortar (1) and planetary ball mill for 30 min (2) and 60 min (3). The inserts show the microstructure images for different $(Cu_{0.5}Ag_{0.5})_7SiS_5I$ ceramic samples.

frequency shift of low-frequency semicircle on EEC is observed. It may be related to the increasing of influence of diffusion ionic processes as well as increasing of ionic relaxation time due to the electronic conductivity decreasing.

Temperature studies have shown that with increasing temperature, the increase of electronic conductivity gradually eliminates the influence of diffusion ionic processes at the boundaries of ceramics crystallites, as evidenced by the decrease of the high-frequency semicircle at 323 K (Fig. 4, curve 2). With further increase of temperature up to 373 K (Fig. 4, curve 3) there is a further reduction of the influence of diffusion ionic processes, which, together with the decrease in the thickness of the double diffusion layer, and the complete disappearance of the high-frequency semicircle.

Fig. 5a shows the dependences of the ionic and electronic components of electrical conductivity on the size of crystallites in $(Cu_{0.5}Ag_{0.5})_7SiS_5I$-based ceramic samples. It is revealed that the decrease in the size of crystallites leads to monotonous decrease of ionic and electronic components of electrical conductivity, while their ratio remains unchanged ($\sigma_{ion}\sigma_{el}$). The decrease in the total electrical conductivity and its ionic and electronic components with decreasing crystallite size 12 μm → 5 μm→ 3 μm, may be associated with an increase in the dispersion of the ceramic material. It increases the number of intercrystallite boundaries, which hinders the efficiency of ion transport and increases the electronic resistance R_e which is responsible for the electronic component of electrical conductivity.

The temperature dependences of the ionic and electronic components of electrical conductivity in the Arrhenius coordinates presents on Fig. 6. The linear behavior of above mentioned
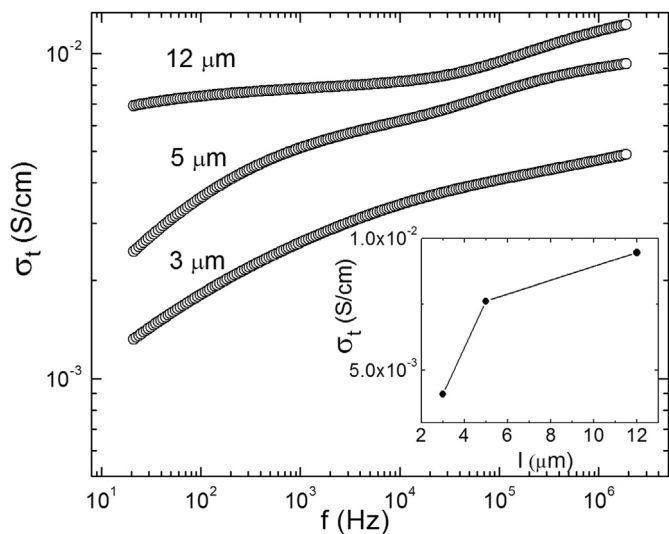
Fig. 3. Frequency dependences of total electrical conductivity at $T = 298$ K for $(Cu_{0.5}Ag_{0.5})_7SiS_5I$ ceramic samples with different sizes of crystallites: 12 μm, 5 μm, and 3 μm. The insert shows the dependence of the total electrical conductivity on the size of crystallites at 100 kHz.

dependences was confirmed the thermoactivating character of electrical conductivity. From the presented temperature de-pendences of the ionic and electronic conductivity the activation energies were determined (Fig. 5b). It is shown that the activation energies of both components of electrical conductivity for $(Cu_{0.5}Ag_{0.5})_7SiS_5I$-based ceramic samples nonlinearly depend on the size of crystallites (рис.5b). Thus, at the transition of the size of crystallites from 12 μm to 5 μm the slight increase of the activation energies of both components of electrical conductivity is observed, whereas at the transition of the size of crystallites from 5 μm to 3 μm the tendency to decrease of the activation energies of both components of electrical conductivity is revealed.

It should be noted that $(Cu_{0.5}Ag_{0.5})_7SiS_5I$-based ceramics are characterized by disordered structure, which is associated with different reasons: (i) structural disordering, caused by the different size of crystallites; (ii) structural disordering, caused by the recrystallization process during annealing; (iii) compositional dis-ordering, caused by the $Cu^+ \leftrightarrow Ag^+$ cationic substitution. The com-bination of the above features in the final case leads to a change of the Nyquist plots for samples with different size of crystallites (Fig. 4) and causes the corresponding behavior of the total electrical conductivity (Fig. 3), its ionic and electronic components (Fig. 5), and its thermoactivation behavior (Fig. 6) for $(Cu_{0.5}Ag_{0.5})_7SiS_5I$-

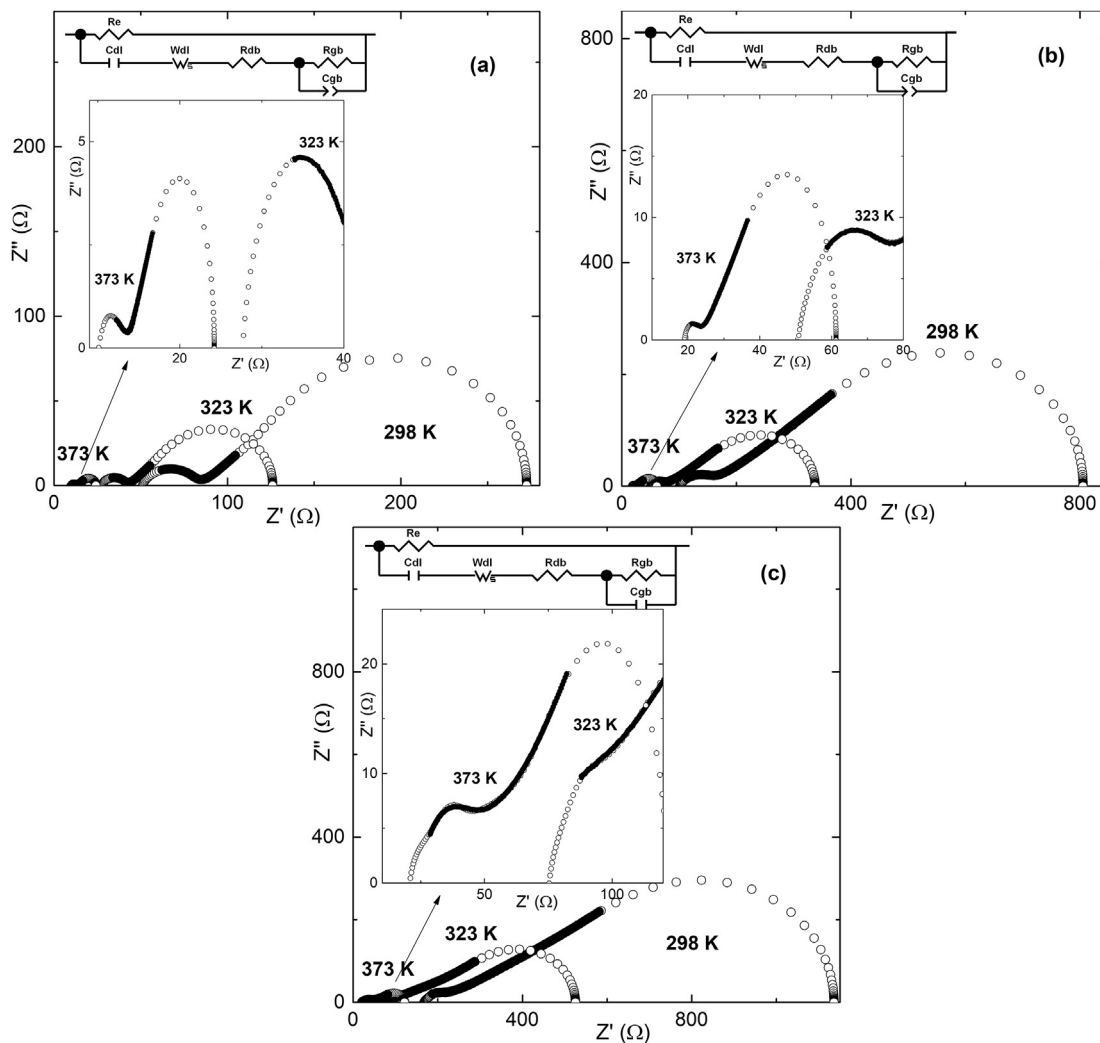**Fig. 4.** EEC and Nyquist plots for $(Cu_{0.5}Ag_{0.5})_7SiS_5I$ ceramic samples with different crystallite sizes: (a) 12 μm; (b) 5 μm; (c) 3 μm for different temperatures. Experimental data correspond to the solid dots, calculated data correspond to the open dots.
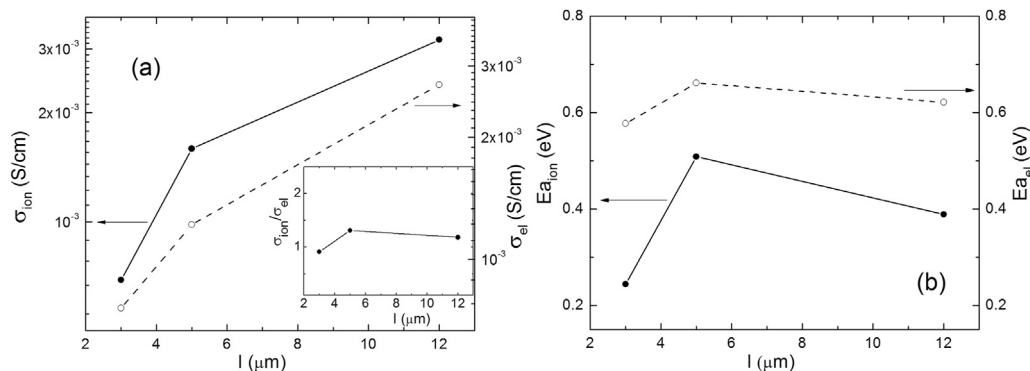
Fig. 5. (a) Dependences of ionic and electronic components of electrical conductivity at $T = 298$ K on the size of crystallites for $(Cu_{0.5}Ag_{0.5})_7SiS_5I$ ceramic samples; the insert shows the dependence of the ratio of the conductivity components on the size of the crystallites; (b) Dependences of the activation energy of ionic and electronic components of electrical conductivity on the size of crystallites for $(Cu_{0.5}Ag_{0.5})_7SiS_5I$ ceramic samples.

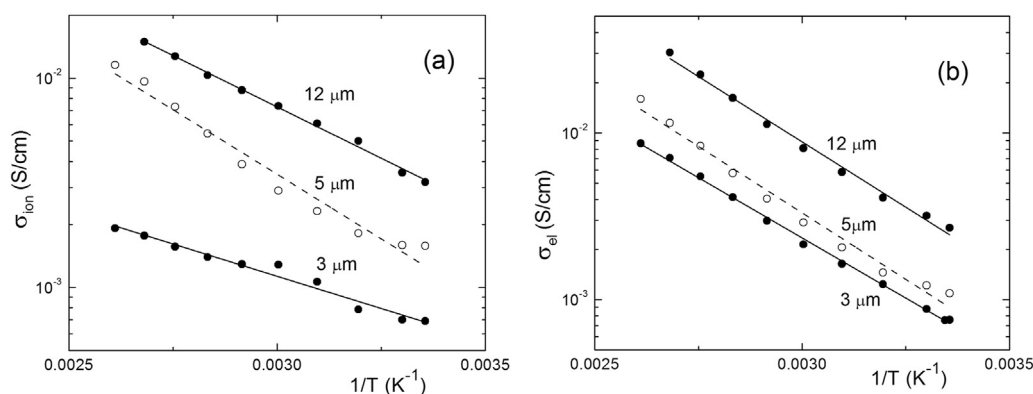**Fig. 6.** Temperature dependences of ionic (a) and electronic (b) components of electrical conductivity for $(Cu_{0.5}Ag_{0.5})_7SiS_5I$ ceramic samples with different sizes of crystallites: 12 μm, 5 μm, and 3 μm.

based ceramics.

Comparison of the values of ionic and electronic conductivities, as well as their ratio for crystal and ceramic samples of $(Cu_{0.5}Ag_{0.5})_7SiS_5I$ solid solution have shown that the ionic conductivity and the ratio σ_{ion}/σ_{el} of ceramic sample with an average crystallite size of 12 μm is slightly greater than that of crystal ones ($\sigma_{ion} = 2.2 \times 10^{-3}$ S/cm and $\sigma_{ion}/\sigma_{el} = 0.9$ for crystal) [25]. Thus, studies show that $(Cu_{0.5}Ag_{0.5})_7SiS_5I$-based ceramics is characterized by high electrical parameters, comparable or even higher than in the corresponding crystals. This, in turn, makes their use in solid ionic devices more promising due to their greater manufacturability and ease of production compared to crystals.

4. Conclusions

The compound of $(Cu_{0.5}Ag_{0.5})_7SiS_5I$ solid solution with the same content of copper and silver atoms was synthesized and three types of ceramic samples were made on its basis by pressing and sintering. Powders of different dispersion were obtained by grinding in an agate mortar as well as in a planetary ball mill. X-ray diffraction spectra showed that during grinding the structure of the argyrodite type is preserved, however, as the particle size decreases, the diffraction bands expand.

Impedance studies for $(Cu_{0.5}Ag_{0.5})_7SiS_5I$ ceramic samples were performed in the frequency range from 10 Hz to 2×10^6 Hz and temperature interval from 292 K to 383 K. With increasing frequency, an increase of the total electrical conductivity and its decrease with decreasing crystallite size were observed. It is revealed that the values of ionic and electronic components are almost equal ($\sigma_{ion} \approx \sigma_{el}$), with decreasing crystallites size they decrease, and their ratio σ_{ion}/σ_{el} remains unchanged. Revealed high values of electrical parameters for $(Cu_{0.5}Ag_{0.5})_7SiS_5I$ ceramics, which are comparable to the values for crystals, make them promising to develop on their basis electrochemical devices.

CRediT authorship contribution statement

I.P. Studenyak: Supervision. **A.I. Pogodin:** Visualization, Investigation. **I.A. Shender:** Visualization, Investigation. **S.M. Bereznyuk:** Software, Validation. **M.J. Filep:** Data curation, Writing - original draft. **O.P. Kokhan:** Conceptualization, Methodology. **P. Kúš:** Writing - review & editing.

Declaration of competing interest

The authors declare that they have no known competing financial interests or personal relationships that could have appeared to influence the work reported in this paper.

Appendix A. Supplementary data

Supplementary data to this article can be found online at https://doi.org/10.1016/j.jallcom.2020.157131.

References

[1] Y. Gogotsi, P. Simon, True performance metrics in electrochemical energy storage, Science 334 (2011) 917−918.

[2] V. Fernao Pires, E. Romero-Cadaval, D. Vinnikov, I. Roasto, J.F. Martins, Power converter interfaces for electrochemical energy storage systems − a review, Energy Convers. Manag. 86 (2014) 453−475.

[3] H. Li, X. Zhang, Z. Zhao, Z. Hu, X. Liu, G. Yu, Flexible sodium-ion based energy storage devices: recent progress and challenges, Energy Storage Mater. 26 (2020) 83−104.

[4] B. Nykvist, M. Nilsson, Rapidly falling costs of battery packs for electric vehicles, Nat. Clim. Change 5 (2015) 329−332.

[5] Z. Wu, Z. Xie, A. Yoshida, Z. Wang, X. Hao, A. Abudula, G. Guan, Utmost limits of various solid electrolytes in all-solid-state lithium batteries: a critical review, Renew. Sustain. Energy Rev. 109 (2019) 367−385.

[6] J.W. Fergus, Ceramic and polymeric solid electrolytes for lithium-ion batteries, J. Power Sources 195 (2010) 4554−4569.

[7] Z. Zhang, Q. Zhang, C. Ren, F. Luo, Q. Ma, Y.-S. Hu, Z. Zhou, H. Li, X.e Huang, L. Chen, A ceramic/polymer composite solid electrolyte for sodium batteries, J. Mater. Chem. 4 (2016) 15823−15828.

[8] Y. Wang, W. Richards, S. Ong, L.J. Miara, J.C. Kim, Y. Mo, G. Ceder, Design principles for solid-state lithium superionic conductors, Nat. Mater. 14 (2015) 1026−1031.

[9] P.-J. Lian, B.-S. Zhao, L.-Q. Zhang, N. Xu, M.-T. Wu, X.-P. Gao, The inorganic sulfide solid electrolytes for all-solid-state lithium secondary batteries, J. Mater. Chem. 7 (2019) 20540−20557.

[10] K.H. Park, D.H. Kim, H. Kwak, S.H. Jung, H.-J. Lee, A. Banerjee, J.H. Lee, Y.S. Jung, Solution-derived glass-ceramic NaI×Na$_3$SbS$_4$ superionic conductors for all-solid-state Na-ion batteries, J. Mater. Chem. 6 (2018) 17192−17200.

[11] M. Tatsumisago, A. Hayashi, Sulfide glass-ceramic electrolytes for all-solid-state lithium and sodium batteries, J. Appl. Glass Sci. 5 (2014) 226−235.

[12] Q. Ma, C.-L. Tsai, X.-K. Wei, M. Heggen, F. Tietz, J.T.S. Irvine, Room temperature demonstration of a sodium superionic conductor with grain conductivity in excess of 0.01 S cm^{-1} and its primary applications in symmetric battery cells, J. Mater. Chem. 7 (2019) 7766−7776.

[13] A. Hayashi, K. Noi, A. Sakuda, M. Tatsumisago, Superionic glass-ceramic electrolytes for room-temperature rechargeable sodium batteries, Nat. Commun. 3 (2012) 856.

[14] R.C. Xu, X.H. Xia, Z.J. Yao, X.L. Wang, C.D. Gu, J.P. Tu, Preparation of Li$_7$P$_3$S$_{11}$ glass-ceramic electrolyte by dissolution-evaporation method for all-solid-state lithium ion batteries, Electrochim. Acta 219 (2016) 235−240.

[15] W.D. Jung, J.-S. Kim, S. Choi, S. Kim, M. Jeon, H.-G. Jung, K.Y. Chung, J.-H. Lee, B.-K. Kim, J.-H. Lee, H. Kim, Superionic halogen-rich Li-argyrodites using in situ nanocrystal nucleation and rapid crystal growth, Nano Lett. 20 (2020) 2303−2309.

[16] L. Zhou, A. Assoud, Q. Zhang, X. Wu, L.F. Nazar, New family of argyrodite thioantimonate lithium superionic conductors, J. Am. Chem. Soc. 141 (2019) 19002−19013.

[17] H. Wang, C. Yu, S. Ganapathy, E.R.H. van Eck, L. van Eijck, M. Wagemaker, A lithium argyrodite Li$_6$PS$_5$Cl$_{0.5}$Br$_{0.5}$ electrolyte with improved bulk and interfacial conductivity, J. Power Sources 412 (2019) 29−36.

[18] H.-J. Deiseroth, S.-T. Kong, H. Eckert, J. Vannahme, C. Reiner, T. Zaiß, M. Schlosser, Li$_6$PS$_5$X: a class of crystalline Li-rich solids with an unusually high Li+ mobility, Angew. Chem. Int. 47 (2008) 755−758.

[19] W.F. Kuhs, R. Nitsche, K. Scheunemann, The argyrodites − a new family of the tetrahedrally close-packed structures, Mater. Res. Bull. 14 (1979) 241−248.

[20] T. Nilges, A. Pfitzner, A structural differentiation of quaternary copper argyrodites: structure − property relations of high temperature ion conductors, Z. Kristallogr. 220 (2005) 281−294.

[21] A.F. Orliukas, E. Kazakevicius, A. Kezionis, T. Salkus, I.P. Studenyak, R.Yu Buchuk, I.P. Prits, V.V. Panko, Preparation, electric conductivity and dielectrical properties of Cu$_6$PS$_5$I-based superionic composites, Solid State Ionics 180 (2009) 183−186.

[22] I.P. Studenyak, V.Yu Izai, V.I. Studenyak, O.V. Kovalchuk, T.M. Kovalchuk, P. Kopčanský, M. Timko, N. Tomašovičová, V. Zavisova, J. Miskuf, I.V. Oleinikova, Influence of Cu$_6$PS$_5$I superionic nanoparticles on the dielectric properties of 6CB liquid crystal, Liq. Cryst. 44 (2017) 897−903.

[23] T. Šalkus, E. Kazakevičius, J. Banys, M. Kranjčec, A.A. Chomolyak, YuYu, . Neimet, I.P. Studenyak, Influence of grain size effect on electrical properties of Cu$_6$PS$_5$I superionic ceramics, Solid State Ionics 262 (2014) 597−600.

[24] I.P. Studenyak, M. Kranjčec, V.Yu Izai, A.A. Chomolyak, M. Vorohta, V. Matolin, C. Cserhati, S. Kökényesi, Structural and temperature-related disordering studies of Cu$_6$PS$_5$I amorphous thin films, Thin Solid Films 520 (2012) 1729−1733.

[25] I.P. Studenyak, A.I. Pogodin, V.I. Studenyak, V.Yu Izai, M.J. Filep, O.P. Kokhan, M. Kranjčec, P. Kúš, Electrical properties of copper- and silver-containing superionic (Cu$_{1-x}$Ag$_x$)$_7$SiS$_5$I mixed crystals with argyrodite structure, Solid State Ionics 345 (2020). P.115183(6).

[26] M.E. Orazem, B. Tribollet, Electrochemical Impedance Spectroscopy, John Wiley & Sons, New Jersey, 2008.

[27] A.K. Ivanov-Schitz, I.V. Murin, Solid State Ionics, Vol, 1, S.-Petersburg Univ. Press, 2000 (in Russian).

[28] R.A. Huggins, Simple method to determine electronic and ionic components of the conductivity in mixed conductors: a review, Ionics 8 (2002) 300−313.